Journal of the Korean Nuclear Society
Volume 33, Number 5, pp.526~538, October, 2001

Fatigue Crack Growth Characteristics of the Pressure Vessel Steel SA 508 Cl. 3 in Various Environments

S. G. Lee and I. S. Kim
Korea Advanced Institute of Science and Technology
373-1, Kusong-dong, Yusong-gu, Taejon, 305-701, Korea

Y. S. Park, J. W. Kim, and C. Y. Park
Korea Electric Power Research Institute
103-16, Munji-dong, Yusong-gu, Taejon, 305-380, Korea

(Received July 6, 2000)

Abstract

Fatigue tests in air and in room temperature water were performed to obtain comparable data and stable crack measuring conditions. In air environment, fatigue crack growth rate was increased with increasing temperature due to an increase in crack tip oxidation rate. In room temperature water, the fatigue crack growth rate was faster than in air and crack path varied on loading conditions. In simulated light water reactor (LWR) conditions, there was little environmental effect on the fatigue crack growth rate (FCGR) at low dissolved oxygen or at high loading frequency conditions. While the FCGR was enhanced at high oxygen condition, and the enhancement of crack growth rate increased as loading frequency decreased to a critical value. In fractography, environmentally assisted cracks, such as semi-cleavage and secondary intergranular crack, were found near sulfide inclusions only at high dissolved oxygen and low loading frequency condition. The high crack growth rate was related to environmentally assisted crack. These results indicated that environmentally assisted crack could be formed by the Electrochemical effect in specific loading condition.

Key Words : enviranmental fatigue, crack growth rate, pressure vessel steel

I. Introduction

In high temperature water environment, the fatigue crack growth behavior of low alloy steels is very different from that in air at ambient temperature [1-3]. The characteristics of the crack growth in water environment are not easily explained by air data trends. And a fast crack growth may be enhanced by cyclic load in combination with environments due to the environmentally assisted crack (EAC). EAC is manifested by the fracture modes of intergranular, cleavage, or brittle striated types [3, 20].

Many researchers and research groups,

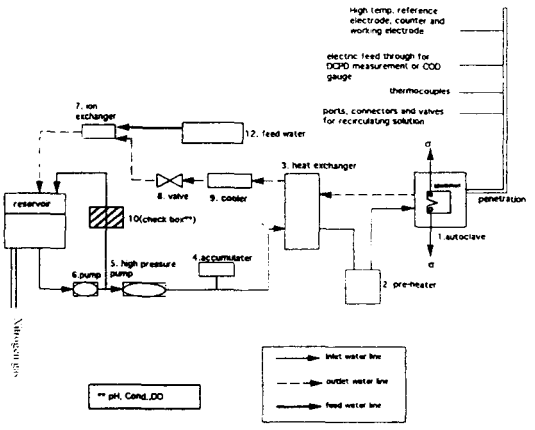

Fig. 1. Schematic Diagram of LWR Simulator ; Max. Flow Rate 7liter/h, Max. Pressure 17MPa

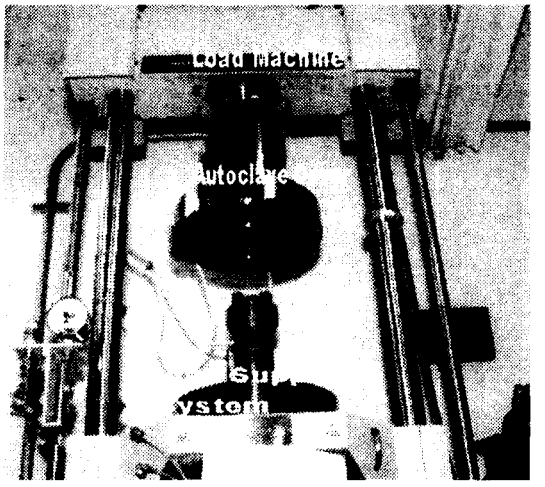

Fig.2. Photograph of LWR Simulator ; Autoclave and Load Frame

especially ICCGR[2,5] (International Cooperative Group on Cyclic Crack Growth Rate), have performed studies on the characteristics of EAC in nuclear pressure boundary material after Kondo' s data reported [1]. The behaviors of the EAC are characterized by water conditions, loading conditions, and material properties. However proposed models and/or mechanisms for EAC [15-21] are still contradictory, since it is difficult to differentiate experimentally what a reaction between anodic (metal dissolution) and cathodic (hydrogen evolution) is critical. Moreover, material processing is also an important variable [2, 3], so it is meaningful to magnify the EAC behavior of a domestic steel in high temperature water.

There are few reported results of domestic vessel steels, especially at the simulated reactor operating conditions. This would mainly result from the short of a test technique and a test system for evaluating fatigue property in simulated nuclear pressure boundary. The objectives of this study are to stabilize the test apparatus and to investigate the fatigue crack properties of the domestic vessel steel in various environments.

2. Experimental Apparatus

Fig. 1 shows a schematic diagram of LWR simulator, which consists of autoclave, water loop and loading machine. Test system was designed to simulate the light water reactor environment for a long period and to monitor crack growth of specimen, and electrochemical parameters. After setting up, the characteristics of the system were confirmed.

2.1. Capacities of LWR Simulator

LWR simulator is composed of an autoclave with 5 liter and INSTRON 8502 as shown in Fig. 2. The type of the autoclave is crucible and metal gasket is applied to seal. The maximum temperature and pressure of water in the autoclave are 340℃ and 170kg/cm^2, respectively. The 5-ton tensile load is able to be applied on a specimen as the maximum load.

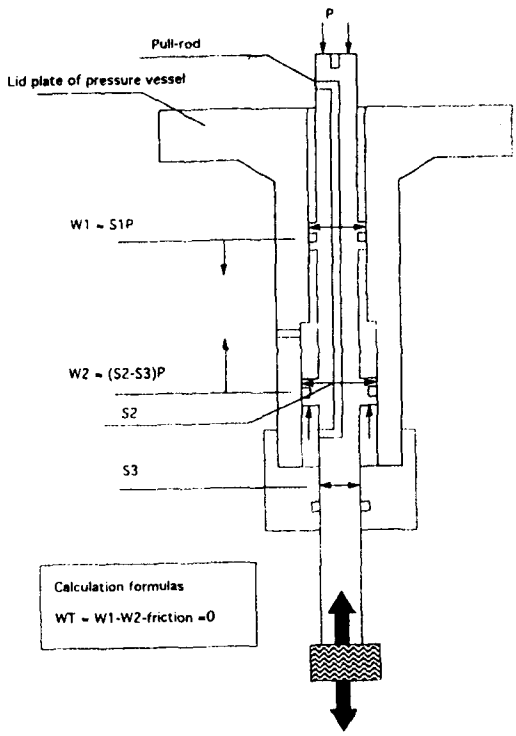

Fig. 3. A Schematic Diagram of the Pressure Balancing Mechanism

Friction between loading rods and sealing parts is compensated by using pressure-balancing mechanism, as shown in Fig. 3. The friction is compensated by pressure difference between upper and lower load chucks. It has been recommended that the temperature and pressure of autoclave should be maintained and the friction between loading rods and seal parts should be minimized [3,4]. In test environment, the friction load was measured with free specimen at various loading conditions. As shown in Fig. 4, the friction load depended on displacement and frequency of actuator. However, it was low enough to meet ICCGR recommendation [3].

The temperature of the autoclave is controlled by a three-band heater with PID method. Several penetrations through autoclave plate were made

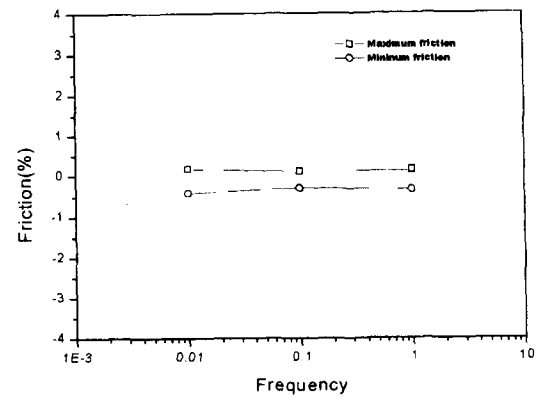

Fig. 4. Results of Friction Between Load Actuator and Seal Part

to monitor crack length, temperature and electrochemical parameters.

The water loop was designed to maintain constant chemical conditions in autoclave, distilled and de-ionized water was continuously fed at 5 liter/h through the test section. To prevent temperature transition, a pre-heater is installed in the loop. An accumulator is used to inhibit impact pulse from pressure pump.

The dissolved oxygen content in water is controlled by nitrogen gas purging. Electrochemical potential of a specimen is monitored by the pressure balancing type external Ag/AgCl reference electrode.

2.2. Crack Length Monitoring System

The change in crack length during loading is monitored in situ using a reversing direct current potential drop (reversing DCPD) method in which a constant current, whose direction is reversed about once per some seconds, is applied to the specimen, and the potential drop across the crack mouth is measured. Many potential readings are averaged, and then relate to crack length through polynomial fits verified by experience. Reversing

Table 1. Composition of SA508Cl. 3

	C	Si	Mn	S	P	Ni	Cr	Mo	Al	Cu	V
(wt/o)	0.21	0.25	1.24	0.002	0.007	0.88	0.21	0.47	0.008	0.03	0.004

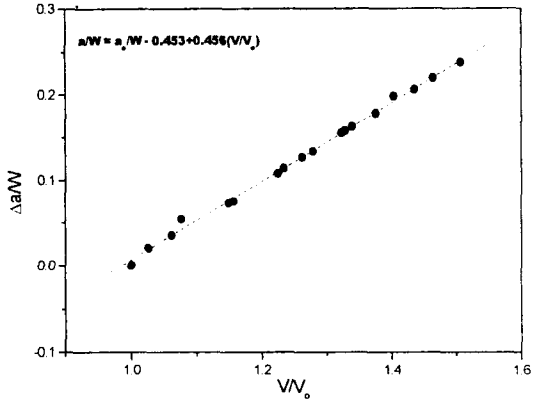

Fig. 5. The Relationship Between Direct Current Potential Drop and Crack Length

DCPD system has some advantages that reduce thermal drift, so potential measurement at high temperature could be stable for a long term [6].

The load train is insulated electrically from the remainder of the autoclave system to prevent Galvanic couples, using Zr/ZrO_2 tube and plate. And electric wires for DCPD system and electrochemical system were sleeved by thermally shrinkable Teflon tube. Correlation between potential drop and crack length was calibrated through a visual method in air environment using a calibration curve shown in Fig. 5.

3. Experimental Procedures

3.1. Material

The SA508 Cl.3 used in this study was a forged pressure vessel steel of 10 inch thick which was produced by Han Jung Co.. The as-received vessel steel had been austenized at 880℃ for 7 hr and water quenched, then tempered for 9 hr at 655 ℃, and air-cooled. The chemical composition and mechanical properties of the steel are given in Table 1 and 2, respectively. 1-inch compact tension specimens were made to test fatigue crack growth in accordance with ASTM E647 [7].

3.2. Fatigue Crack Growth Test

Fatigue crack growth rate tests were conducted under various environmental and mechanical conditions in linear elastic range [7]. Pre-cracking of the fatigue specimen was conducted in room temperature air environment. Fatigue tests in argon, air and room temperature water environment were performed to achieve comparable data and stable crack measuring conditions. Test in argon environment was performed with purging high purity argon gas at a pressure of 400kPa.

In 288℃ and 10MPa water condition, experiments were conducted to study the effect of dissolved oxygen (DO) content and frequency on fatigue properties of SA508Cl.3. Avoiding the effects of pre-cracked regions on the specimen surface in air environment, data were taken after 2.5mm crack increment. After each test, the specimen was broken in liquid nitrogen, then its fractured surface was observed by scanning electron microscopy(SEM). Also post-test crack length correction was conducted.

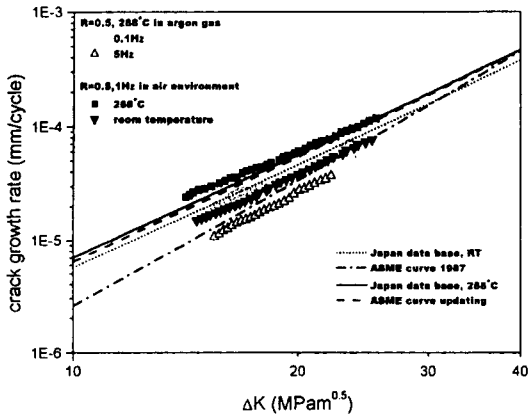

Fig . 6. Fatigue Crack Growth Rate of SA508 Cl.3 Steel in Argon and Air Environment

4. Results and Discussion

4.1. Fatigue Crack Growth Rate in Inert and Air Environments

Crack growth rates of SA508Cl.3 steel in argon and air environments were shown and compared with ASME reference curve [8] and Japanese database [9] in Fig. 6. The crack growth rate property of the steel was similar to that in Japanese database rather than that shown in the ASME reference curve. For the ASME reference curve, it was not considered the effects of temperature but only R-ratio (P_{max}/P_{min}) [8]. However in Japanese database, it was specified by temperature and R-ratio [9]. So it would be very important to consider the effect of temperature in constructing the database of fatigue crack growth rate.

In argon and air environment, the fatigue crack growth rate of SA508 alloy followed Paris' law in this study. At the tested load range, the crack growth rate increased by two or three times at 288℃ than at room temperature in air environment. While crack growth rate at 288℃ in argon environment decreased to lower than that at room temperature in air environment. This trend of crack growth rate may result from changes of crack tip plasticity and oxidation rate.

Even though the size of crack tip plasticity is lower in air than in vacuum [11], it was reported that crack growth rates in air are generally higher than those in vacuum [11,12]. And there were no significant effects of temperature on crack growth rate of low alloy steel in vacuum [11,12]. In this study, the crack growth rate was decreased at similar loading condition in argon environment where oxygen pressure was low, as shown in Fig. 6. So it is reasonable to assume that contributions of changes of crack tip plasticity should be negligible and that contributions of the changes of oxidation rates would be dominant.

To establish a connection between the rate of crack growth and that of oxidation, an obvious route is to study activation energies for oxidation assisted fatigue crack growth. For a thermally activated process

$$\frac{da}{dN} = C\exp(-\frac{Q}{RT}) \quad (1)$$

where C is a rate constant and Q is the activation energy.

In this study, Q of fatigue crack growth was calculated by the following equation.

$$(\frac{da}{dN})_{288} / (\frac{da}{dN})_{RT} = \exp(\frac{Q}{298R} - \frac{Q}{581R}) = 2\sim3 \quad (2)$$

The activation energy of fatigue crack growth rate from equation (2) was about 5~6kJ/mol which is much smaller than that of oxidation rate on surface of low alloy steels [12]. According to King [12], the small activation energy of crack growth rate could be due to a different mechanism from metal removal with oxidation which is applicable at higher than 300℃. And they proposed that two different environmental mechanisms in air operate along with the mechanical condition according to

temperature.

At higher temperatures than 300℃ , an oxidation enhances crack growth rates by metal removal at crack tip due to high oxidizing environment, freshly exposed as existing oxide films spall during crack opening. In this region, the activation energy of crack growth rate is equivalent to that of metal oxidation rate. However, at lower temperatures, the oxidation is not sufficient to remove a significant thickness of metal. So it is reasonable that crack growth rate would be determined by an irreversibility of slip [12], because an aggravation of mechanical irreversibility could be dominant in low oxidizing environment where high modulus oxide repels dislocations, or a hindrance of surface rejoining owing to the presence of the oxide film at crack tip forms.

In fractography study, there was little difference of fracture surfaces between at room temperature and 288℃, and crack grew in a transgranular mode with ductile striated type, which is a typical feature of fatigue crack growth of low alloy steels [10,12]. This implies that the cracking mechanism at 288℃ is similar to that at room temperature.

By considering the activation energy of fatigue crack growth rate with that of oxidation rate on metal surface, the crack growth rate of SA508Cl.3 was to increase through oxidation induced irreversibility of slip at crack tip in air environment as temperature increases from room temperature to 288℃.

4.2. Fatigue Crack Growth Rate in pH 4.7 Water at Room Temperature

The fatigue crack growth rate of SA508Cl.3 in acidic solution at room temperature is presented in Fig. 7, and was reproducible at the repeated condition. Crack growth rate was more enhanced in water environment than in air environment, the

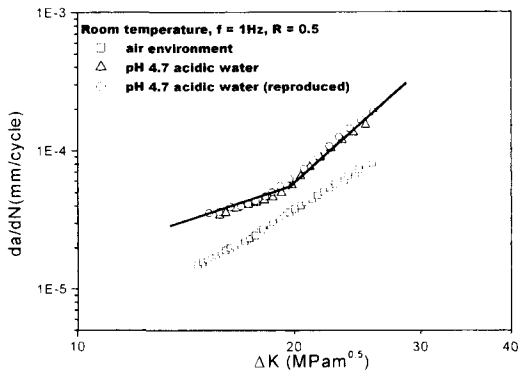

Fig. 7. Fatigue Crack Growth Rate of SA508Cl. 3 Steel at Room Temperature in pH 4.7 Water

enhancement of crack growth rate in water environment may result from the combinations of chemical reactions and stress at crack tip. And load dependency, which is the slope of curve in Fig. 7, was changed at 20MPam$^{0.5}$ in water environment. Difference of load dependency could be resulted from changes of crack paths in water environment as load condition changes, or crack closure from corrosion product wedging [13,14]. It is expected that closure effect is minor in this study, since R-ratio is high enough to exclude it [13,14].

The slope of crack growth rate vs. stress intensity factor range curve in water environment was about 1.74 at ΔK values lower than 20MPam$^{0.5}$, and 3.67 at ΔK values higher than 20MPam$^{0.5}$. This implies that crack advance is less dependent on a mechanical driving force and is mainly affected by a chemical driving force at ΔK values lower than 20MPam$^{0.5}$ in room temperature water. The slope was constant at the tested load range in air environment, and cracking mechanism in air environment was a ductile striated type at the tested load range.

In the specimen tested in water, the change of load dependency with load increase was related

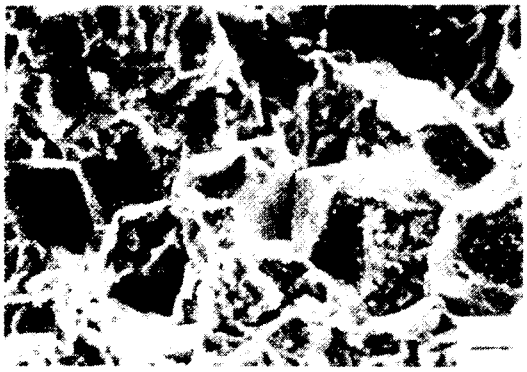

(a)

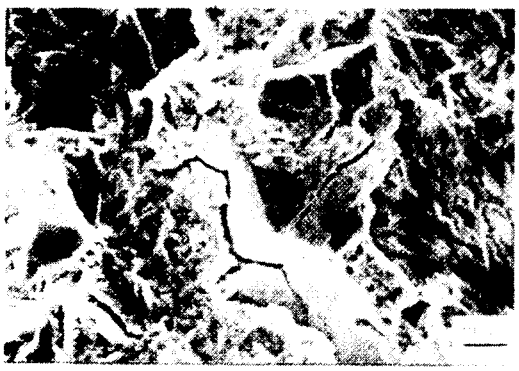

(b)

(c)

Fig . 8. The Fracture Surfaces Tested in Room Temperature Water; (a) mixed mode of transgranular and intergranular, (b) mixed mode of transgranular and intergranular, (c) transgranular mode

with change of crack path from intergranular at low load to transgranular at high load. The fractography results are represented in Fig. 8. Crack grew along prior austenite grain boundaries at 15MPam$^{0.5}$, as represented in Fig. 8(a). At 20MPam$^{0.5}$, intergranular facets were diminished as shown in Fig. 8(b). At 25MPam$^{0.5}$, crack grew along transgranular facets with brittle striated type as represented in Fig. 8(c).

A relationship between the crack path change and the load condition is well correlated through considering size of crack tip plasticity. The size of crack tip plasticity is about 40μm at 15MPam$^{0.5}$ [29] which is equivalent to an average size of prior austenite grain. As load increases, the size of crack tip plasticity increases and is proportional to $\frac{\Delta K^2}{\sigma_{y,s}E}$. In this result the intergranular crack is dominant at smaller size of crack tip plasticity and fraction of intergranular crack becomes negligible when the size of crack tip plasticity becomes two times of prior austenite grain.

In aqueous environment there are several reactions at crack tip, such as metal dissolution, formation/fracture of protective film, reduction of hydrogen ion or oxygen gas, and so on. These reactions are involved in crack growth with mechanical conditions, such as, stress intensity factor, frequency, and R-ratio. Based on the reactions and mechanics, two basic mechanisms, dissolution-controlled and hydrogen-induced, have been generally proposed [15]. In the former process the crack propagation is controlled by anodic dissolution of the metal at the crack tip, whereas in the latter process the mechanical separation at the crack tip is facilitated by hydrogen embrittlement. Both mechanisms for crack propagation depend on the same rate-determining parameters, i.e. oxide formation/fracture, which makes it difficult to differentiate experimentally

between these mechanisms.

Although it was difficult to determine the exact mechanism from the results of this study, two types of environmentally assisted crack were found, since grain boundary was a crack path at low load condition in water environment while it was not in air environment. And there is still an environmental effect on transgranular fatigue-crack-growth rate with brittle striated type when the fraction of intergranular crack growth becomes negligible as shown in Fig. 8(c).

Grain boundary would be electrochemically activated by dissolving itself and/or trapping hydrogen in water environment since it is chemically and energetically unstable. The electrochemically-activated sites would be crack paths when a mechanical driving force for crack growth is small. Because a stress is more concentrated by a notch effect of the dissolution site in view of anodic dissolution mechanism [16-19] or a binding energy is decreased by trapped hydrogen in view of hydrogen embrittlement mechanism [20-22].

When mechanical driving force is sufficient, the electrochemically-activated sites were less important because mechanically activated sites could be sufficient. In addition, a direction of maximum driving force is normal to load so that crack grew along transgranular with the brittle striated type which enhanced crack growth rate in water environment than in air environment at high load.

In conclusion, fatigue of SA508Cl.3 at room temperature water, environmentally assisted cracks were found which were intergranular facets and transgranular crack with brittle striated type. The types of environmentally assisted cracks were controlled by the size of prior austenite grains and the loading conditions in room temperature water environment.

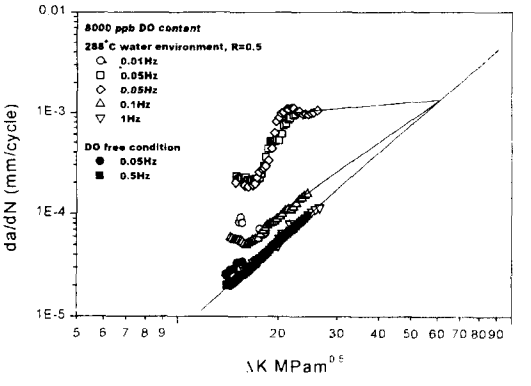

Fig. 9. Fatigue Crack Growth Rate of SA508Cl.3 at 288℃ in High Pure Water

3. Fatigue Crack Growth Behavior in High Temperature Water Environment

3.1. Trend of Crack Growth Rate

Crack growth rate in pure water at high temperature and high pressure was represented in Fig. 9. It is mainly dependent on DO content. Crack growth rate was enhanced only at high DO content depending on test frequency, while there was little difference between air and water results at low DO content.

At high DO content, crack growth rate was increased with decreasing frequency up to a critical value in range of 0.01Hz and 0.05Hz. At 1Hz the enhancement of crack growth rate were diminished and similar to that at air condition.

3.2. Fractography Results

At air saturated water condition, there existed bands on local regions of fracture surface due to

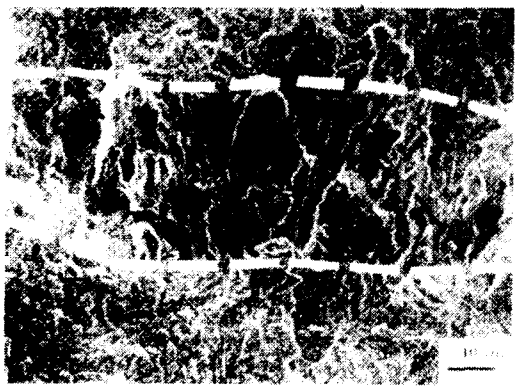

(a)

(b)

Fig. 10. Fracture Surface Tested in High Temperature Water at Air Saturated Condition; (a) band fromation, (b) brittle facet and secondary intergranular crack at hole

the difference of oxide scale properties between inside and outside of them as represented in Fig. 10(a). The bands started at holes which would be dissolution sites of inclusions. The band lengths were related to size and quantity of the holes and test conditions. There were environmentally assisted cracks around the hole, such as secondary intergranular crack and fan shaped crack as shown in Fig. 10(b). Bands were not found in low DO content and/or high frequency conditions although the holes were found as shown in Fig. 11.

Fig. 11. Fracture Surface Tested in High Temperature Water at DO Free Condition

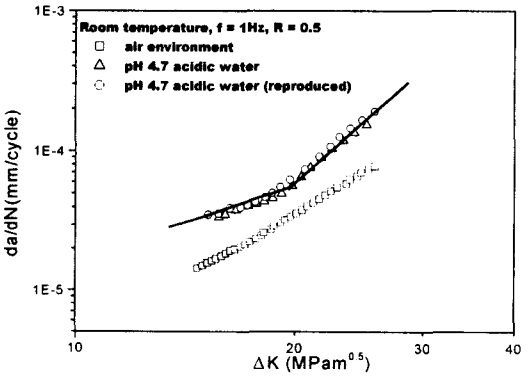

(a)

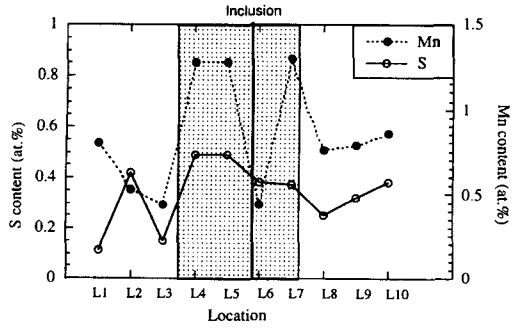

(b)

Fig. 12. Results of Chemical Analysis Around Hole from Dissolving Inclusion

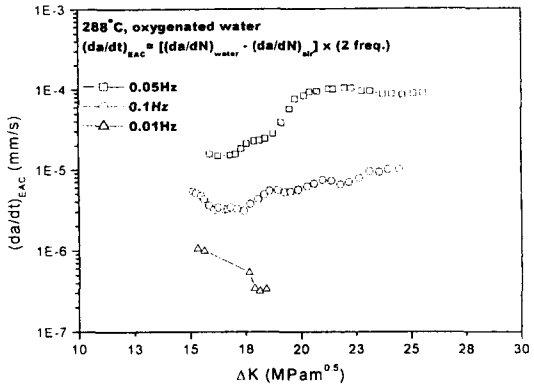

Fig. 13. Crack Growth Rate Calculated by Assumption of Superposition$(da/dt)_{EAC}$: a true crack growth rate of corrosion fatigue

Surface analysis on bands was preformed with EDX (Energy Dispersive Spectrometer) to examine the identity of hole. The results were represented in Fig. 12. In the band region a trace of sulfur and Mn was detected and oxygen content was less than that outside the band region. This fact means that the holes were dissolved sites of Mn-S inclusions and the oxide composition was affected by sulfur ion.

3.3. The Effects of MnS, DO Content and Frequency

As shown in fractography study and in crack growth rate data, major parameters affecting on cracking were MnS, dissolved oxygen and loading frequency. These parameters control the crack tip conditions interacting with each other [3, 23-27].

As shown in fractography results, dissolved MnS inclusion is a source of sulfur ion at crack tip which remains with forming oxide scale at the band in oxygenated water. At the high-oxygenated water, an activity of sulfur ion at crack tip is higher than at oxygen free water since there is a potential drop between crack mouth and tip [23,27]. The activity of sulfur at crack tip is main rate determining parameter, since it controls the rate of metal dissolution and hydrogen evolution. This is the cause that crack growth rate increases with the dissolved oxygen content.

Table 2. Mechanical Properties of SA508Cl.3 at Room Temperature

0.2% Yield Strength	448Mpa
Tensile Strength	593 MPa
Elongation	29%
Reduction of Area	74%
Charpy Energy	138J
RTNDT	-30℃
Microhardness	180 ~ 208Hv

However, the crack growth rate was not enhanced at 1Hz loading frequency and the band around dissolution site was not found although the potential drop exists. This implies that frequency affects the sulfur activity at crack tip and environmental effect was nearly diminished at 1Hz. In addition, crack growth was less enhanced at 0.01Hz condition than at 0.05Hz. It seemed there is a critical frequency between 0.01Hz and 0.05Hz where the crack growth rate is maximized. Effect of loading frequency could be resulted because loading frequency affects fracture rate of oxide film, a pumping velocity of crack surfaces and a diffusion time of sulfur ion [23, 26].

To magnify pure environmental effects, a true crack growth rate of the corrosion fatigue was calculated by subtracting the crack growth rate in air from that in water, and the result was represented in Fig. 13. The calculation was made with assuming superposition [28]. From these results at beginning of test, the true crack growth rate of 0.1Hz and 0.01Hz tests decreased as a

mechanical driving force increased, while that of 0.05Hz test is stable. For the case of 0.1Hz, the sulfur activity would be decreased by the pumping velocity of crack surface although frequency of oxide film rupture is high. For the case of 0.01Hz, although pumping velocity is very low the true crack growth rate was not increased. This is mainly due to the fact that a rate of oxide film rupture is very low and a diffusion time of sulfur ion from crack tip to bulk solution is sufficient at 0.01Hz. For these reasons the crack growth rate would decrease as (K increases at 0.01Hz and 0.1Hz, in addition, the critical frequency where crack growth rate is maximized was ranged around 0.05Hz.

4. Conclusions

The effects of environments on fatigue crack growth rate of SA508 steel was examined in air, room temperature water, and high temperature water. In particular, the effect of dissolved oxygen content and loading frequency on the fatigue crack growth rate of the pressure vessel steel SA508Cl.3 was investigated in high temperature water. Results obtained are summarized as follows:

(1) LWR simulator was successfully set up. Crack measurement system was established and crack growth rate was coincident with fractographic features.

(2) In air environment, crack growth rate depended on oxidation at crack tip. Crack growth rate of SA508Cl.3 increased through oxidation at crack tip in air environment as temperature increases from room temperature to 288℃. Activation energy was about 5kJ/mole.

(3) In fatigue tests of SA508Cl.3 at room temperature water, environmentally assisted cracks were found which were intergranular facets and transgranular cracks with brittle striated type. The types of environmentally assisted cracks were controlled by the size of prior austenite grains and the loading condition in room temperature water.

(4) Crack growth rate in high temperature water was understood by considering the effects of inclusion, dissolved oxygen and loading frequency. Especially the critical frequency where crack growth rate is maximized was ranged between 0.01 and 0.05Hz. In addition, crack growth rate increased due to MnS dissolution and sulfur activity at the crack tip.

Acknowledgments

This work was partially supported by Brain Korea 21 program.

References

1. T. Kondo, T. Kikuyama, H. Nakajima, M. Shindo, and R. Nagasaki, "Corrosion fatigue of ASTM A302B steel in high temperature water, the simulated nuclear reactor environment," Proc. Conf. On Corr. Fati. on Chemistry, Mechanics and Microstructure, NACE-2, p539 (1971).
2. R.L Jones, P. Hurst, and P. M. Scott, "Round Robin/Collaborative Programme," Int. J. Pres. Ves. & Piping, Vol.40, p 375 (1989).
3. J. H. Bulloch, " A fractogrphic assessment of sulphide inclusion distributions and their influence in promoting environmentally assisted crack growth in ferritic pressure vesses steels," Int. J. Pres.. Ves. & Piping Vol.56, p149(1993).
4. T. Kondo, Private communication, (1995).
5. P. M Scott, "Data acquisition," Int. J. Pres. Ves. & Piping Vol.40, p335 (1987).
6. W. R. Catlin, D. C. Lord, T. A. Prater and L. F. Coffin, "The reversing D-C electrical potential

method," ASTM STP 877, p67, (1985).
7. Annual Book of ASTM Standards, E647-93
8. ASME Boiler and Pressure Vessel Code, Sec. XI. (1988).
9. H. Kobayashi, H. Nakamura, K. Kasai, M. saito, T. Funada, K. Shibata, and K. Iida, " Construction of a fatigue crack growth database for nuclear component ferritic steels in Japan and its statistical analysis," Int. J. Pres. Ves. & Piping Vol.44, p67(1990).
10. A. D. Wilson, "Fractographic characterization of the effect of inclusions on fatigue crack propagation," ASTM STP 733, p166(1981).
11. L. A. James, "The fatigue crack propagation behavior of ASTM A533B steel tested in vacuo at LWR operating temperatures," Nuclear Eng. and Design Vol.105, p243(1988).
12. J. E. King, and P. J. Cotterill, " Role of oxides in fatigue crack propagation," Mat. Sci. and Tech., Vol.6, p19(1990).
13. K. Endo, K. Komai, and T. Shikida, " Crack growth by stress assisted dissolution and threshold characteristics in corrosion fatigue of a steel," ASTM 801, p81(1983).
14. R. van der Velden, H. L. Ewalds, W. A. Schultze, and P. Punter, "Anomalous fatigue crack growth retardation in steels for offshore applications," ASTM STP 801, p64 (1983).
15. L. Hagn, "Life prediction methods for aqueous environments," Mat. Sci. and Eng. A103, p193(1988).
16. F. P. Ford, "Quantitative prediction of environmentally assisted cracking," Corr., Vol. 52, p 375(1996).
17. P. L. Andresen, and F. P. Ford, "Fundamental modeling of environmental cracking for improved desing and lifetime evaluation in BWRs," Int. J. Pres. Ves. & Piping, Vol.59 p 61, (1994) .
18. F. P. Ford, D. F. Taylor, P. L. Andresen, and R. G. Ballinger, EPRI NP 5064M Project 2006-6 final report (1987).
19. P. L. Andresen, and L. M. Young, "Crack tip microsampling and growth rate measurements in low alloy steel in high temperature water," Corr. Sci. Vol.51, p223 (1995).
20. K. Toerroenen, and W. H. Cullen, "Effect of light water reactor environments on fatigue crack growth rate in reactor pressure vesses steels," ASTM STP 770, p 460(1982).
21. H. Haenninen, K. Toerroenen, M. Kemppainen, and S. Salonen, "On the mechanisms of environment sensitive cyclic crack growth of nuclear reactor pressure vessel steels," Corr. Sci. Vol.23, p663 (1983).
22. B. J. Berkowitz, and F. H. Heubaum, "The role of hydrogen in sulfide stress cracking of low alloy steels," Corrosion Vol.40, p240 (1984).
23. P. L. Andresen, " Modeling of water and material chemistry effects on crack tip chemistry and resulting crack growth kinetics," International Symp. on Env. Deg. of mat. In Nuclear Power Systems-water reactors p301(1988).
24. W. A. Van Der Sluys, and R. H. Emanuelson, "Fatigue crack growth in reactor pressure vessel materials and light water reactor environments," Nuclear Eng. And Design Vol.119, p379 (1990).
25. Y. Katada, N. Nagata, and S. Sato, "Effect of dissolved oxygen concentration on fatigue crack growth behavior of A533B steel in high temperature water," ISIJ International Vol.33, p877 (1993).
26. H. En-Hou, and K. Wei, "Chemical and electrochemical conditions within corrosion fatigue cracks," Corr. Sci. Vol.35, p599 (1993).
27. H. Hanninen, M. Vulli, W. H. Cullen, "Study

of corrosion products on Fatigue surfaces of Pressure vessel steels tested in PWR Env. by using X-Ray photoelectron and AUGER electron spectroscopies," International Symp. On Env. Deg. of mat. In Nuclear Power Systems-water reactors, p289 (1988).

28. J. P. Thomas and R.P. Wei, " corrosion fatigue crack growth of steels in aqueous solutions," Mat. Sci. and Eng. A159, p205(1992).
29. R. W. Hertzberg, " Deformation and fracture mechanics of engineering materials", 3rd John Wiley &Sons, p529(1989).